THE INCORPORATION OF LUNG SURFACTANT SPECIFIC PROTEIN SP-B INTO LIPID MONOLAYERS AT THE AIR-FLUID INTERFACE: A GRAZING INCIDENCE X-RAY DIFFRACTION STUDY

K.Y.C. LEE*, J. MAJEWSKI**, T.L. KUHL§, P.B. HOWES¶, K. KJAER¶, M.M. LIPP§, A.J. WARING#, J.A. ZASADZINSKI§, G.S. SMITH**

*Department of Chemistry, The University of Chicago, Chicago, IL 60637 kayeelee@rainbow.uchicago.edu

**Manuel Lujan Jr. Neutron Scattering Center, Los Alamos National Laboratory, Los Alamos, NM 87545

§Department of Chemical Engineering, University of California, Santa Barbara, CA 93106-5080

¶Condensed Matter Physics and Chemistry Department, Risø National Laboratory, DK-4000, Roskilde, Denmark

#Department of Pediatrics, Martin Luther King Jr./Drew Medical Center and UCLA, Los Angeles, CA 90095

ABSTRACT

Grazing incidence x-ray diffraction (GIXD) measurements were performed to determine the effects of SP-B_{1-25}, the N-terminus peptide of lung surfactant specific protein SP-B, on the structure of palmitic acid (PA) monolayers. In-plane diffraction shows that the peptide fluidizes a portion of the monolayer, but does not affect the packing of the residual ordered phase. This implies that the peptide resides in the disordered phase, and that the ordered phase is essentially pure lipid. The quantitative insights afforded by this study lead to a better understanding of the lipid/protein interactions found in lung surfactant systems.

INTRODUCTION

Lung surfactant (LS), a complex mixture of lipids and proteins, lines the alveoli, and is responsible for the proper functioning of the lung [1]. LS works both by lowering the surface tension inside the lungs to reduce the work of breathing, and by stabilizing the alveoli through varying the surface tension as a function of alveolar volume. To accomplish this, the LS mixture must adsorb rapidly to the air-fluid interface of the alveoli after being secreted. Once at the interface, it must form a monolayer that can both achieve low surface tensions upon compression and vary the surface tension as a function of the alveolar radius. Insufficient levels of surfactant, due to either immaturity in premature infants, and disease or trauma in adults, can result in respiratory distress syndrome (RDS), a potentially lethal disease in both populations.

LS consists primarily of the saturated dipalmitoylphosphatidylcholine (DPPC), unsaturated phosphatidylcholines, along with significant amounts of unsaturated and anionic phospholipids such as phosphatidylglycerols (PGs), lesser amounts of anionic lipids such as palmitic acid (PA), and neutral components like cholesterol. LS also contains four lung surfactant-specific proteins, known as SP-A, -B, -C, and -D. Of the four, SP-B and SP-C are small, amphipathic proteins believed to be important for the surface activity of LS. Although the complete roles of SP-B and SP-C are not yet fully understood, they are known to be essential for the proper functioning of LS in vivo and in replacement surfactants for the treatment of RDS. SP-B in particular has been shown to greatly increase the activity of LS lipids both in vitro and in vivo. It has also been demonstrated that simple peptide sequences based on the amino terminus of SP-B possess the full activity of the native protein [2-5].

Mat. Res. Soc. Symp. Proc. Vol. 590 © 2000 Materials Research Society

Pure DPPC can form monolayers that attain surface tensions near zero values on compression; in the context of LS, this feature of DPPC definitely helps reduce the work of breathing. However, DPPC adsorbs and respreads slowly as a monolayer under physiological conditions, rendering it by itself not an ideal LS candidate [1, 6-8]. The unsaturated and anionic lipids present in natural LS and added to many replacement surfactants are believed to enhance the adsorption and respreading of DPPC [6-8]. PA, for example, is one of the three compounds added to exogenous surfactant in Survanta (8.5 w/w; Ross Laboratory, Columbus, Ohio) and Surfactant TA (8.5% w/w; Tokyo Tanabe) used to treat premature infants with neonatal RDS. PA by itself collapses at relatively low surface pressures, however, the addition of full length SP-B or its amino-terminus peptide, SP-$B_{1\text{-}25}$, to monolayers of PA results in much higher monolayer collapse pressures (lower surface tension values) than those of either PA or SP-B alone. This suggests that a synergistic effect between PA and SP-B may result in the retention of both the lipid and the protein in the primarily DPPC monolayer upon compression [9].

To determine how the SP-$B_{1\text{-}25}$ protein incorporates itself into the PA monolayer, we have carried out a series of GIXD experiments on both pure PA and mixed PA/SP-$B_{1\text{-}25}$ monolayers at the air-water interface at different surface pressures. Our findings give us the first quantitative information on the effect of SP-$B_{1\text{-}25}$ on the packing of the PA monolayer, and helps to pinpoint the location of the peptide in the lipid matrix.

EXPERIMENT

Palmitic acid, PA, (Sigma Chemical Co., St. Louis, MO; > 99% pure) was used as obtained. All subphases were prepared using 18.2 MΩ•cm Millipore water obtained from a Milli-Q UV Plus system (Millipore Corp.). Stock spreading solutions were made with either pure chloroform (for PA) or 4:1 vol/vol chloroform-methanol (for SP-$B_{1\text{-}25}$). Spreading solution were made by mixing aliquots of the stock solutions to obtain the desired concentration.

The synthetic peptide based on the first 25 amino acids of the NH_2-terminal sequence of SP-B, SP-$B_{1\text{-}25}$, shown in Fig. 1, was synthesized by the solid state method using a Fmoc strategy with an Applied Biosystems 431A peptide synthesizer. Details of the synthesis have been published elsewhere [10].

1 + ++ + 25

NH_2–FPIPLPYCWLCRALIKRIQAMIPKG-COOH

Figure 1. Amino acid sequence of the N-terminal truncated model peptide $SP\text{-}_{B1\text{-}25}$, with the positively charged residues indicated with a plus sign.

All synchrotron x-ray measurements were performed with the liquid surface diffractometer [11, 12] at the BW1 (undulator) beam line [13] at HASYLAB, DESY (Hamburg, Germany). A thermostated Langmuir trough, equipped with a Wilhelmy balance for measuring the surface pressure (π), and a barrier for surface pressure control, was mounted on the diffractometer. In a typical experiment, a monolayer was first spread using a microsyringe at the desired temperature. At least 30 minutes was allowed for complete solvent evaporation before the two-dimensional film was compressed to the desired surface pressure. The film was then held at this surface pressure throughout the experiment. The trough was enclosed in a sealed, helium-filled canister where the oxygen level was constantly monitored.

The synchrotron x-ray beam was monochromated to a wavelength of λ=1.303 Å by Laue reflection from a Be (200) monochromator crystal. By tilting the reflecting planes out of the vertical plane, the monochromatic beam could be deflected down to yield a glancing angle with

the horizontal liquid surface. The x-ray beam was adjusted to strike the surface at an incident angle of $\alpha_i = 0.11° = 0.85\ \alpha_c$, where α_c is the critical angle for total external reflection. At this angle the incident wave is totally reflected, while the refracted wave becomes evanescent, traveling along the liquid surface. Such a configuration maximizes surface sensitivity [14]. The dimensions of the incoming x-ray beam footprint on the liquid surface were approximately 5 mm X 50 mm or 1 mm X 50 mm.

In three-dimensional (3D) crystals, Bragg diffraction takes place only when the scattering vector $\boldsymbol{Q}$ coincides with $\{h,k,l\}$ points of the reciprocal 3D lattice, giving rise to Bragg spots (h, k, l are the Miller indices). In our two-dimensional (2D) systems and at surface pressures of interest, the PA monolayers are a mosaic of 2D crystals with random orientation about the direction normal to the subphase, and can therefore be described as 2D powders. Due to the lack of a vertical crystalline repeat, there is no restriction on the scattering vector component Q_z along the direction normal to the crystal: Bragg scattering from a 2D crystal extends as continuous Bragg rods through the reciprocal space [11, 15, 16]. The scattered intensity is measured by scanning over a range of horizontal scattering vectors $Q_{xy} \sim (4\pi/\lambda)\sin(2\theta_{xy}/2)$, where $2\theta_{xy}$ is the angle between the incident and diffracted beam. The Bragg peaks, resolved in the Q_{xy}-direction, are obtained by integrating the scattered intensity over all the channels along the Q_z-direction in the position sensitive detector (PSD). Conversely, the Bragg rod profiles are obtained by integrating, after background subtraction, for each PSD channel, the scattered intensity across a Bragg peak. The angular positions of the Bragg peaks allow the determination of the spacings $d = 2\pi/Q_{xy}$ for the 2D lattice. From the line shapes of the peaks, it is possible to determine the 2D crystalline coherence length, L (the average distance in the direction of the reciprocal lattice vector Q_{xy} over which crystallinity extends). The intensity distribution along the Bragg rod can be analyzed to determine the direction and magnitude of the molecular tilt.

RESULTS

Experiments were carried out at 16 °C on a pure water subphase. On pure water, 16 °C is well below the triple point of a PA monolayer [10, 17]. The triple point denotes the unique temperature and surface pressure in the pure component phase diagram where the condensed (LC), liquid-expanded (LE) and gaseous (G) phase all coexist in equilibrium. As the LE phase does not exist below the triple point temperature, a LC film is guaranteed at low non-zero surface pressures. These conditions thus made it possible to probe any fluidizing effect of the peptide on the PA monolayer. GIXD measurements were made on pure PA as well as mixed PA/20 wt% SP-$B_{1\text{-}25}$ monolayers, with the films held at different surface pressures. In all cases, the pure PA experiments gave a "baseline" for comparison with the mixed monolayer.

The diffraction pattern obtained for pure PA monolayers at π = 15 mN/m and π = 30 mN/m are shown in Fig. 2a. At π = 15 mN/m, two Bragg peaks are observed at Q_{xy} = 1.45 Å^{-1} and Q_{xy} = 1.50 Å^{-1}, the corresponding coherence lengths are 160 Å and 450 Å, respectively. The observation of precisely two Bragg peaks in the 2D powder pattern is indicative of a rectangular unit cell [18]. Previous work on fatty acid monolayers has also shown that in the rectangular *S*, *L2*, *L2'* phases these monolayers yield two in-plane reflections: $\{1,1\}_{rect}$ and $\{0,2\}_{rect}$ [19-22]. The integrated intensity of the Bragg peak at Q_{xy} = 1.45 Å^{-1} peak is roughly twice that of the Q_{xy} = 1.50 Å^{-1} peak. This higher intensity results from coincident $\{1,1\}_{rect}$ and $\{1,-1\}_{rect}$ reflections, and thus leads to the assignment of the $\{1,1\}_{rect}$ reflection to the Q_{xy} = 1.45 Å^{-1} peak and the $\{0,2\}_{rect}$ reflection to the Q_{xy} = 1.50 Å^{-1} peak. The calculated d-spacings, d_{11} = 4.33 Å (d_{xy} =

$2\pi/(Q_{xy})$ and d_{02} = 4.19 Å, give rise to a rectangular unit cell with axes $|a|$ = 5.06 Å ($1/|a|^2 = (1/d_{11}^2 - 1/(2d_{02})^2)$ and $|b|$ = 8.38 Å, and an area per chain, A_{15}, of 21.2 Å^2 (two molecules per unit cell of area = 42.4 Å^2).

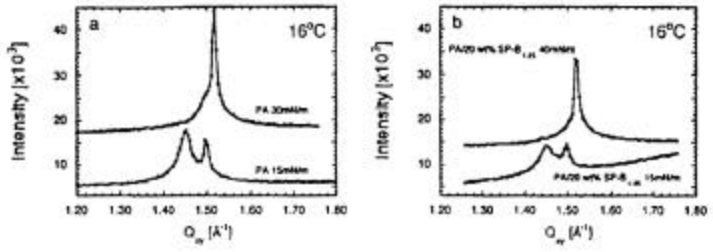

Figure 2.Bragg peaks from GIXD on pure water at 16 °C of (a) a pure PA film at 15 mN/m and 30 mN/m; (b) a mixed PA/20 wt% SP-$B_{1\text{-}25}$ film at 15 mN/m and 40 mN/m. For clarity, the high pressure data have been offset vertically.

The $\{0,2\}_{rect}$ Bragg rod has its maximum in the intensity profile at Q_z = 0 Å^{-1} (Bragg rod profiles not shown), which indicates that the molecular axis lies in a plane perpendicular to the b axis. We analyzed the $\{1,1\}_{rect}$ and $\{0,2\}_{rect}$ Bragg rod intensity profiles (data not shown) by approximating the PA molecule by a cylinder with constant electron density [11]. Our results show that the molecule has a tilt of ~ 21° towards the nearest neighbor (along unit vector a) direction, and the effective thickness (thickness projected on the surface normal) of the monolayer is 20.5 Å.

When the system is compressed to 30 mN/m, the two Bragg peaks at 15 mN/m collapse into one (see Fig. 2a), indicating a transition to a hexagonal lattice. The scattering vector for the single Bragg peak, indexed as $\{1,0\}_{hex}$ is Q_{xy} = 1.52 Å^{-1}, with an average coherence length of 470 Å, which is a significant increase over the coherence length of the $\{1,1\}_{rect}$ reflections at 15 mN/m. The hexagonal lattice has a d-spacing of 4.13 Å and the unit cell dimension (an intermolecular distance) $a_H = d/\cos 30° = 4.77$ Å. The interfacial area per chain, A_{30}, is reduced to 19.7 Å^2. The position of the intensity maximum of the Bragg rod (Q_z ~ 0 Å^{-1}; data not shown) implies ~ 0° tilt of the molecules at 30 mN/m. Using the areas obtained for surface pressures of 15 mN/m (A_{15}) and 30 mN/m (A_{30}) we find once again the tilt angle of the chain at 15 mN/m, t_{15} = arccos (A_{30}/A_{15}) ~ 21°. This agrees well with that obtained from fits to the $\{1,1\}_{rect}$ and $\{0,2\}_{rect}$ Bragg rods above. The quantitative information shows that an increase in surface pressure primarily causes a decrease in the area per PA molecule due to a decrease in molecular tilt, while maintaining the molecular packing in the plane normal to the molecules.

The Bragg peaks obtained for the lipid/peptide mixed monolayers at 15 mN/m and 40 mN/m are shown in Fig. 2b. At 15 mN/m, two Bragg peaks resulting from $\{1,1\}_{rect}$ and $\{0,2\}_{rect}$ reflections are observed at Q_{11} = 1.45 Å^{-1} and Q_{02} = 1.50 Å^{-1}, with coherence lengths L_{11} = 130 Å and L_{02} = 425 Å. The d-spacings have values d_{11} = 4.33 Å and d_{02} = 4.20 Å, indicating a rectangular unit cell with axes $|a|$ = 5.05 Å and $|b|$= 8.40 Å with an interfacial area per molecule of 21.2 Å^2. Similar to the pure PA case, the $\{0,2\}_{rect}$ Bragg rod has its maximum intensity at Q_z ~ 0

$Å^{-1}$, and the profile of the $\{1,1\}_{rect}$ reflection gives a tilt angle of 20.4° towards the nearest neighbor (along unit vector *a*) direction. Comparing these results with those for pure PA, it is apparent that the presence of SP-$B_{1\text{-}25}$ does not affect the lipid packing of the condensed phase. The unit cell, the coherence lengths, and the molecular tilt found in the condensed phase of PA are all preserved in this mixed system. This suggests that the peptide is completely excluded from the condensed region of the film, consistent with fluorescence imaging [10, 17]. As a PA monolayer at 16 °C is well below the triple point and should be in a pure LC phase at 15 mN/m, our results indicate that incorporating the peptide into the monolayer creates a disordered phase whose structure cannot be probed by the GIXD techniques.

Corroborative evidence of this disordered phase can be found by the drop (by a factor of *ca.* 2.1) in integrated intensity observed when SP-$B_{1\text{-}25}$ is present (see Figs. 2a and 2b). Since GIXD is only sensitive to the ordered phase, this decrease in scattering intensity suggests that a disordered phase occupies *ca.* 50 percent of the monolayer surface area, which is qualitatively consistent with our fluorescence microscopy findings [10, 17].

At 40 mN/m, the mixed film exhibits a single Bragg peak at Q_{xy} = 1.52 $Å^{-1}$ with a coherence length of 450 Å. As was observed without the peptide, the condensed phase of the monolayer assumes a hexagonal packing with ~ 0° molecular tilt. The *d*-spacing is 4.13 Å, with an intermolecular separation of 4.77 Å and an area per molecule of 19.8 $Å^2$. These lattice parameters are identical (within experimental errors) to the pure PA monolayers at 30 mN/m. This implies that the condensed phase of the film at this elevated pressure is only made up of PA molecules. A direct comparison at 40 mN/m is not possible because the pure PA film collapses below 40 mN/m. Unlike the low surface pressure case, the integrated intensity found in this case is only slightly lower than that in pure PA at 30 mN/m, the ratio being *ca.* 1.3. It should be noted that the two cases are at different pressures (30 mN/m without protein; 40 mN/m with protein), that may also account for the smaller decrease in the scattering intensity. Nonetheless, the smaller decrease is consistent with fluorescence images that show a smaller fluid phase at higher surface pressures [10, 23].

CONCLUSIONS

GIXD measurements were used to investigate the influence of the truncated LS peptide, SP-$B_{1\text{-}25}$, on the packing of PA monolayers at the air-water interface. From the GIXD we infer that on pure water subphase, the peptide is incorporated into the disordered phase of the PA monolayer. The insertion of the peptide leads to a reduced amount of ordered phase in the film, as reflected by a decrease in scattering intensity in our GIXD data. This reduction in scattering intensity is particularly apparent at 16 °C. Below the triple point of the PA film, a disordered phase does not exist at non-zero surface pressures in pure PA films; the disordered phase that occurs when peptide is present points to the fluidizing capabilities of SP-$B_{1\text{-}25}$. This finding corroborates our fluorescence microscopy data, which show that a disordered phase is created when SP-$B_{1\text{-}25}$ is present in the PA monolayer.[10, 17]

Although SP-$B_{1\text{-}25}$ induces a disordered phase in the monolayer, our GIXD data show that the peptide does not affect the molecular packing of the ordered phase. Within experimental errors, films with and without SP-$B_{1\text{-}25}$ have identical packing parameters. This suggests that the peptide is completely excluded from the ordered phase of the film, and hence must reside in the disordered portion of the monolayer. It should be pointed out that the lattice parameters obtained here for PA and the mixed PA/SP-$B_{1\text{-}25}$ monolayers are similar to those found in longer chain fatty acids.

ACKNOWLEDGMENTS

We gratefully acknowledge beam time at HASYLAB at DESY, Hamburg, Germany, and funding by the programs DanSync (Denmark) and TMR of the European Community (Contract ERBFMGECT950059). K.Y.C.L. is grateful for the support from the Camille and Henry Dreyfus New Faculty Award (NF-98-048), the March of Dimes Basil O'Connor Starter Scholar Research Award (5-FY98-0728), the Searle Scholars Program/The Chicago Community Trust (99-C-105), and the American Lung Association (RG-085-N). J.A.Z. and M.M.L. were supported by NIH Grant HL51177. A.J.W. was supported by NIH Grant HL55534. The Manuel Lujan Jr., Neutron Scattering Center is a national user facility funded by the United States Department of Energy, Office of Basic Energy Sciences - Materials Science, under contract number W-7405-ENG-36 with the University of California. This work was also supported in part by the MRSEC Program of the National Science Foundation under Award Numbers DMR-9808595 (The University of Chicago) and DMR96-32716 (University of California, Santa Barbara).

REFERENCES

1. D. L. Shapiro and R. H. Notter, *Surfactant Replacement Therapy*, Alan R. Liss, New York, 1989.
2. A. Waring, W. Taeusch, R. Bruni, J. Amirkhanian, B. Fan, R. Stevens and J. Young, Peptide Research **2**, p. 308-313 (1989).
3. A. Takahashi, A. Waring, J. Amirkhanian, B. Fan and W. Taeusch, Biochim. Biophys. Acta **1044**, p. 43-49 (1990).
4. L. M. Gordon, S. Horvath, M. Longo, J. A. Zasadzinski, H. W. Taeusch, K. Faull, C. Leung and A. J. Waring, Protein Sci. **5**, p. 1662-1675 (1996).
5. M. M. Lipp, K. Y. C. Lee, A. J. Waring and J. A. Zasadzinski, Science **273**, p. 1196-1199 (1996).
6. N. Mathialagan and F. Possmayer, Biochim. Biophys. Acta **1045**, p. 121-127 (1990).
7. A. Cockshutt, D. Absolom and F. Possmayer, Biochim. Biophys. Acta **1085**, p. 248-256 (1991).
8. M. Longo, A. Waring and J. Zasadzinski, Biophys. J. **63**, p. 760-773 (1992).
9. M. Longo, A. Bisagno and J. A. Zasadzinski, Science **261**, p. 453-456 (1993).
10. M. M. Lipp, K. Y. C. Lee, J. A. Zasadzinski and A. J. Waring, Biophys. J. **72**, p. 2783-2804 (1997).
11. J. Als-Nielsen and K. Kjaer in *Phase Transitions in Soft Condensed Matter*, edited by T. Riste and D. Sherrington (Plenum, New York, 1989), p. 113-138.
12. J. Majewski, R. Popovitz-Biro, W. Bouwman, K. Kjaer, J. Als-Nielsen, M. Lahav and L. Leiserowitz, Chem. Eur. J. **1**, p. 302-309 (1995).
13. R. Frahm, J. Weigelt, G. Meyer and G. Materlik, Rev. Sci. Instrum. **66**, p. 1677-1680 (1995).
14. P. Eisenberger and W. C. Marra, Phys. Rev. Lett. **46**, p. 1081 (1981).
15. J. Als-Nielsen, D. Jacquemain, K. Kjaer, F. Leveiller, M. Lahav and L. Leiserowitz, Phys. Rep. **246**, p. 251-313 (1994).
16. K. Kjaer, Physica B **198**, p. 100-109 (1994).
17. M. M. Lipp, K. Y. C. Lee, J. A. Zasadzinski and A. J. Waring, Science **273**, p. 1196-1199 (1996).
18. D. Jacquemain, F. Leveiller, S. Weinbach, M. Lahav, L. Leiserowitz, K. Kjaer and J. Als-Nielsen, J. Am. Chem. Soc. **113**, p. 7684 (1991).
19. K. Kjaer, J. Als-Nielsen, C. A. Helm, P. Tippman-Krayer and H. Möhwald, J. Phys. Chem. **93**, p. 3200-3206 (1989).
20. B. Lin, M. C. Shih, T. M. Bohanon, G. E. Ice and P. Dutta, Phys. Rev. Lett **65**, p. 191-194 (1990).
21. R. M. Kenn, C. Böhm, A. M. Bibo, I. R. Peterson, H.Möhwald, J. Als-Nielsen and K. Kjaer, J. Phys. Chem. **95**, p. 2092-2097 (1991).
22. V. M. Kaganer, H. Möhwald and P. Dutta, Rev. Modern Phys. **71**, p. 779-819 (1999).
23. K. Y. C. Lee, M. M. Lipp, J. A. Zasadzinski and A. J. Waring, Colloids and Surfaces A **28**, p. 225-242 (1997).